

Oxidative Stress-mediated Apoptosis

THE ANTICANCER EFFECT OF THE SESQUITERPENE LACTONE PARTHENOLIDE*

Received for publication, April 19, 2002, and in revised form, July 26, 2002
Published, JBC Papers in Press, July 31, 2002, DOI 10.1074/jbc.M203842200

Jing Wen, Kyung-Ran You, So-Youn Lee, Chang-Ho Song[‡], and Dae-Ghon Kim[§]

From the Division of Gastroenterology and Hepatology, Departments of Internal Medicine and [‡]Anatomy Research Institute for Clinical Medicine, Chonbuk National University Medical School and Hospital, Chonju, Chonbuk 561-712, Republic of Korea

The sesquiterpene lactone parthenolide, the principal active component in medicinal plants, has been used conventionally to treat migraines, inflammation, and tumors. However, the antitumor effects of parthenolide and the mechanism(s) involved are poorly understood. We found that parthenolide effectively inhibits hepatoma cell growth in a tumor cell-specific manner and triggers apoptosis of hepatoma cells. Parthenolide triggered apoptosis in invasive sarcomatoid hepatocellular carcinoma cells (SH-J1) as well as in other ordinary hepatoma cells at 5–10 μM concentrations and arrested the cell growth (at G_2/M) at sublethal concentrations (1–3 μM). During parthenolide-induced apoptosis, depletion of glutathione, generation of reactive oxygen species, reduction of mitochondrial transmembrane potential, activation of caspases (caspases-7, -8, and -9), overexpression of *GADD153* (an oxidative stress or anticancer agent inducible gene), and subsequent apoptotic cell death was observed. This induced apoptosis could be effectively inhibited or abrogated by an antioxidant *N*-acetyl-L-cysteine, whereas L-buthionine-(*S,R*)-sulfoximine enhanced it. Furthermore, stable overexpression of *GADD153* sensitized the cells to apoptosis induced by parthenolide, and this susceptibility could be reversed by transfection with an antisense to *GADD153*. Parthenolide did not alter the expression of Bcl-2 or Bcl-X_L proteins during apoptosis in hepatoma cells. Oxidative stress may contribute to parthenolide-induced apoptosis and to *GADD153* overexpression in a glutathione-sensitive manner. The sensitivity of tumor cells to parthenolide appears to result from the low expression level of the multifunctional detoxification enzyme glutathione *S*-transferase π . Finally, parthenolide and its derivatives may be useful chemotherapeutic agents to treat these invasive cancers.

Sesquiterpene lactones are isolated from extracts of Mexican-Indian medicinal plants and have been widely used in indigenous medical practices, including treatment of migraines

(1, 2), inflammation (3), and tumors (4, 5). Parthenolide, the major sesquiterpene lactone found in medicinal plants such as feverfew (*Tanacetum parthenium*), is known to inhibit interleukin 1- and tumor necrosis factor α -mediated NF- κ B activation, which is responsible for its anti-inflammatory activity (6, 7). Parthenolide has been reported to inhibit NF- κ B by targeting the I κ B kinase complex (7). Parthenolide also exerts an anti-inflammatory activity by inhibiting the expression of inducible cyclooxygenase, proinflammatory cytokines (8), and inducible nitric-oxide synthase (9). In contrast, the cytotoxic and antitumor effects of sesquiterpene lactones have not been well studied because of their low potency. Recently it has been reported that parthenolide inhibits the *in vitro* growth of tumor cells in a cytostatic fashion, and it has been proposed that if their selectively cytotoxic or cytostatic actions against tumor cells can be established, sesquiterpene lactones may represent a new class of cancer chemotherapeutic drugs (10).

Sarcomatoid changes of epithelial neoplasms (carcinomas with spindle-cell components) occur in many organs and histologic types. Sarcomatoid elements in liver cancers are derived from dedifferentiation of hepatocellular carcinoma or cholangiocarcinoma. Although the incidences of spindle-cell hepatocellular carcinoma and cholangiocarcinoma are less than 10% (11, 12) and ~5% (13), respectively, the prognosis for patients with sarcomatoid liver carcinoma is worse than for those with ordinary carcinoma because of the aggressive intrahepatic spreading and the frequent metastasis of sarcomatous cells (12). Thus, we have established a sarcomatoid hepatocellular carcinoma cell line (designated as SH-J1) and have searched for agents that arrest their growth and/or induce their apoptosis. Intriguingly, we have now observed that parthenolide effectively inhibits the proliferation and induces the apoptosis of those sarcomatoid hepatocellular carcinoma cells as well as other ordinary hepatoma cells. The underlying mechanism for the antitumor effects of parthenolide seems to be mediated by oxidative stress. This oxidative stress may subsequently be associated with overexpression of *GADD153*, a growth arrest and DNA damage-inducible gene.

MATERIALS AND METHODS

Growth Inhibition and Cytotoxic Cell Death Assay—Chang liver cells and human hepatoma cell lines, including Hep 3B, PLC/PRF/5, and SK-HEP-1, were obtained from the American Type Culture Collection (ATCC) (Manassas, VA). The sarcomatous SH-J1 cells were established in our laboratory (14). To determine the effects on growth, cells were cultured on coverslips and treated with the indicated concentrations of parthenolide or vehicle (Me₂SO) in Dulbecco's modified Eagle medium (Invitrogen) supplemented with 10% fetal bovine serum for 48 h. The cells were fixed with 4% paraformaldehyde in 0.1 M sodium phosphate buffer (pH 7.6) and were then stained with the Diff-Quick stain set (Dade Diagnostics of P. R. Inc., Aguada, Puerto Rico). To measure cytotoxic cell death, the cells were cultured in 6-cm culture dishes and

* This work was supported in part by grants from the 21C Frontier Human Genome Project, the Ministry of Science and Technology, Republic of Korea, and Korean Research Foundation Grant 001-F00138. The costs of publication of this article were defrayed in part by the payment of page charges. This article must therefore be hereby marked "advertisement" in accordance with 18 U.S.C. Section 1734 solely to indicate this fact.

§ To whom correspondence should be addressed: Division of Gastroenterology and Hepatology, Dept. of Internal Medicine, Chonbuk National University Medical School and Hospital, 634-18 Keumam-dong, Dukjin-ku, Chonju, Chonbuk 561-712, South Korea. Tel.: 82-63-250-1681; Fax: 82-63-254-1609; E-mail: daeghon@moak.chonbuk.ac.kr.

exposed to the indicated concentrations of parthenolide. Cell death was determined by trypan blue dye assay, and the percentage of apoptotic cells was evaluated by Hoechst 33258 (Sigma) staining. At least 200 cells were counted for each time point, and all counting was done in a blinded fashion.

Assay for Inhibition of [³H]Thymidine Incorporation—SH-J1 cells were plated in 96-well flat-bottom microtiter plates (Nalge Nunc International, Naperville, IL) at a density of 10³ cells/well and treated with 1–3 μM parthenolide in medium for 48 h. The cells were labeled with 1 μCi [³H]thymidine/well (specific activity, 5 Ci/mmol; Amersham Biosciences) for 16 h at 37 °C and then harvested on fiberglass filter paper strips with a multiple automated sample harvester (Inotech, Dottikon, Switzerland). Each sample was lysed hypotonically, and radioactivity was measured in a Tri-Carb 4530 liquid scintillation counter (Packard Instrument Company).

Flow Cytometry—Measurements of cell cycle distribution and apoptotic/hypodiploid cells were performed using a modification of the technique described previously (15). For synchronization, the cells were treated with 0.5 μg/ml nocodazole (Calbiochem) to induce M block for 16 h, washed, and incubated in the presence or absence of 3 μM parthenolide. Data were analyzed as single-parameter frequency histograms in an SFIT model. The sub-G₁ fraction was estimated by gating hypodiploid cells in the DNA histogram using a C-30 program.

Detection of DNA Fragmentation—SH-J1 cells (1 × 10⁶) were seeded in 6-cm Petri dishes and allowed to settle and attach. Cells were treated with the indicated concentrations of parthenolide for 48 h. For analysis of genomic DNA, cells were harvested and collected together with nonattached cells in the supernatant. Cells were resuspended in 0.5 ml of lysis buffer (50 mM Tris-HCl, 100 mM EDTA, 0.5% sodium dodecyl sulfate (pH 8.0) containing 0.1 mg/ml RNase A. After incubation at 37 °C for 30 min, extracts were treated with 1 mg/ml proteinase K for an additional 16 h at 37 °C. DNA was extracted with phenol/chloroform and then with chloroform and precipitated with ethanol and sodium acetate, and 5 μg of DNA was separated on a 2% agarose gel. DNA in the gel was stained with ethidium bromide, visualized under UV light, and photographed.

Measurement of Reactive Oxygen Species (ROS)¹ and Mitochondrial Transmembrane Potential (ΔΨ_m)—The intracellular generation of ROS was measured using the oxidation-sensitive fluorescein 5,6-carboxy-2',7'-dichlorofluorescein diacetate (DCFH-DA) (Molecular Probes, Eugene, OR). For measurement of ΔΨ_m, cells were treated with 10 μM parthenolide for the indicated times. 5,5',6,6'-Tetraethylbenzimidazocarbocyanine iodide (JC-1) (Molecular Probes) was added to the medium at 5 μg/ml, and incubation was continued in the dark for 15 min (16). Stained cells were harvested, washed once in phosphate-buffered saline, and analyzed by flow cytometry. A BD Biosciences FACScan was used to analyze a minimum of 10,000 cells/sample. Forward and side scatter were used to gate the viable population of cells. At relatively high ΔΨ_m the dye JC-1 forms J-aggregates, which emit at 590 nm, in the red/orange range of visible light (FL-2 channel). However, in the absence of or at low ΔΨ_m, JC-1 exists as a monomer, remaining in the cell but emitting at 527 nm, in the green range (FL-1 channel).

Northern Blot Analysis—Cells were cultured in Dulbecco's modified Eagle's medium with 10% fetal bovine serum until they were 60% confluent at which time they were treated with 5 μM parthenolide for 48 h. Total RNA was extracted from treated or untreated cells using phenol and guanidine thiocyanate solution (Tri Reagent; Molecular Research Center Inc., Cincinnati, OH) following the manufacturer's instructions. RNAs were then fractionated by electrophoresis on 1.0% agarose gels containing formaldehyde and transferred to membranes. Northern blot analysis was performed as described previously (16). The blots were stripped and then rehybridized with a glyceraldehyde-3-phosphate dehydrogenase (*GAPDH*) probe to normalize the amount of RNA loaded.

Transfection—Transfection of the *GADD153* gene into SH-J1 cells was performed using an expression plasmid vector encoding human *GADD153* cDNA or control pcDNA3. The construct of the *GADD153* expression vector was made by ligating human *GADD153* (a gift from

Dr. Nikki J. Holbrook, NIA, National Institutes of Health, Baltimore, MD) with pcDNA3 at each *Bam*HI/*Xho*I site in the sense orientation. To generate the antisense *GADD153* expression vector, human *GADD153* was PCR-amplified with the forward primer containing the *Xba*I restriction enzyme site (5'-GCTCTAGAGGGCTGCAGAGATGGC-3') and the reverse primer containing the *Eco*RI restriction enzyme site (5'-GGAATTCGGGACTGATGCTCCCA-3'). The PCR-amplified *GADD153* double strand DNA was ligated to pcDNA3 at the *Xba*I/*Eco*RI site in the antisense orientation. Transfections were carried out using Lipofectin (Invitrogen) according to the manufacturer's protocol. *GADD153*-transfected and neo-transfected cells were selected in the presence of 600 μg/ml G418 for 2–3 weeks. Finally, individual colonies were isolated using cloning rings, expanded, and assayed for expression of the transfected gene by Northern analysis and by Western analysis.

Luciferase Assay—pGADD-LUC, a hamster *GADD153* promoter-driven luciferase reporter construct, was a gift from Dr. Nikki J. Holbrook (17). Cells were transfected with the pGADD-LUC construct using Lipofectin (Invitrogen) as noted above. Cells were plated at 2 × 10⁴ cells/well in 24-well plates, and 18 h later, the cells were incubated at 37 °C with 500 ng of GADD-LUC plasmid and 50 ng of pRL-TK plasmid (Promega, Madison, WI) in the presence of Lipofectin for 16 h. The cells were then replenished with complete medium and treated with equitoxic levels of parthenolide. The cells were lysed in 120 μl of lysis buffer at the indicated time intervals and stored at –20 °C until measurement. Luciferase activity was measured using the dual luciferase reporter Assay system (Promega) as instructed by the manufacturer and normalized by *Renilla* luciferase activity.

Glutathione (GSH) Assay—Reduced glutathione was measured using a colorimetric assay kit (OXIS International, Inc., Portland, OR). Cells were treated with either parthenolide alone or in combination with the glutathione precursor *N*-acetyl-L-cysteine (NAC) for 48 h or with the glutathione depleting agent L-buthionine-(*S,R*)-sulfoximine (BSO). Cells treated with BSO were incubated overnight and then treated with parthenolide after washing for 48 h. The homogenate was centrifuged at 3000 × *g*, 4 °C for 10 min, and its supernatant was used for GSH measurement according to the manufacturer's instruction. The cell pellet dissolved in 1 M NaOH was used for the measurement of protein content (18). The GSH content was expressed as nmol/mg of protein or percent of the control.

Cell Lysis and Immunoblotting—Cell lysis and immunoblotting were performed as described previously (18). Cytosolic extracts were prepared from cells in lysis buffer (10 mM PIPES (pH 7.4), 10 mM KCl, 2 mM MgCl₂, 1 mM dithiothreitol, 5 mM ethylene glycol-bis(β-aminoethyl ether) *N,N,N',N'*-tetraacetic acid, 25 μg/ml leupeptin, 40 mM β-glycerophosphate, and 1 mM phenylmethylsulfonyl fluoride). Cells were homogenized with a Dounce homogenizer, and lysis was confirmed by microscopy. Nuclei were collected by centrifugation through 30% sucrose (800 × *g*, 10 min at 4 °C), mitochondria were collected at 10,000 × *g* for 20 min at 4 °C, and the remaining cell membranes were removed by centrifugation at 100,000 × *g* for 45 min at 4 °C, as described previously. The supernatant (S-100 fraction) was used as the cytosolic extract. After adjustment for protein concentration, 30 μg of each cell lysate was boiled in Laemmli buffer and resolved by 15% SDS-PAGE before immunoblot analysis with antibody against cytochrome *c* (Pharmingen). Signals were detected using an ECL Western blotting kit (Amersham Biosciences). The mouse anti-poly(ADP-ribose)polymerase (PARP) monoclonal antibody (C2-10), rabbit anti-caspase-3 polyclonal antibody, mouse anti-caspase-6 monoclonal antibody (B93-4), mouse anti-caspase-7 monoclonal antibody (B94-1), rabbit anti-caspase-8 polyclonal antibody (B9-2), and mouse anti-caspase-9 monoclonal antibody (B40) were purchased from Pharmingen. The mouse anti-Bcl-2 monoclonal antibody (Ab-1) and mouse anti-Bcl-X_L monoclonal antibody (H-5) were obtained from Calbiochem and from Santa Cruz Biotechnology, Inc. (Santa Cruz, CA), respectively.

Statistical Analysis—All data were entered into Microsoft Excel 5.0. GraphPad Software was used to perform paired *t* tests. All *p* values of less than 0.05 were considered to be statistically significant.

RESULTS

Inhibition of Cell Growth and Induction of Apoptosis by Parthenolide—To determine whether parthenolide inhibits cell proliferation, SH-J1 cells were cultured on coverslips and exposed to parthenolide at different concentrations (0–10 μM) for 48 h. The cells were fixed and stained with the Diff-Quick stain set, and cell numbers were histocytologically counted. Parthe-

¹ The abbreviations used are: ROS, reactive oxygen species; ΔΨ_m, mitochondrial transmembrane potential; DCFH-DA, 5,6-carboxy-2',7'-dichlorofluorescein diacetate; JC-1, 5,5',6,6'-tetraethylbenzimidazocarbocyanine iodide; GAPDH, glyceraldehyde-3-phosphate dehydrogenase; GSH, glutathione; NAC, *N*-acetyl-L-cysteine; BSO, L-buthionine-(*S,R*)-sulfoximine; PARP, poly(ADP-ribose)polymerase; GST, glutathione *S*-transferase; PIPES, 1,4-piperazinediethanesulfonic acid.

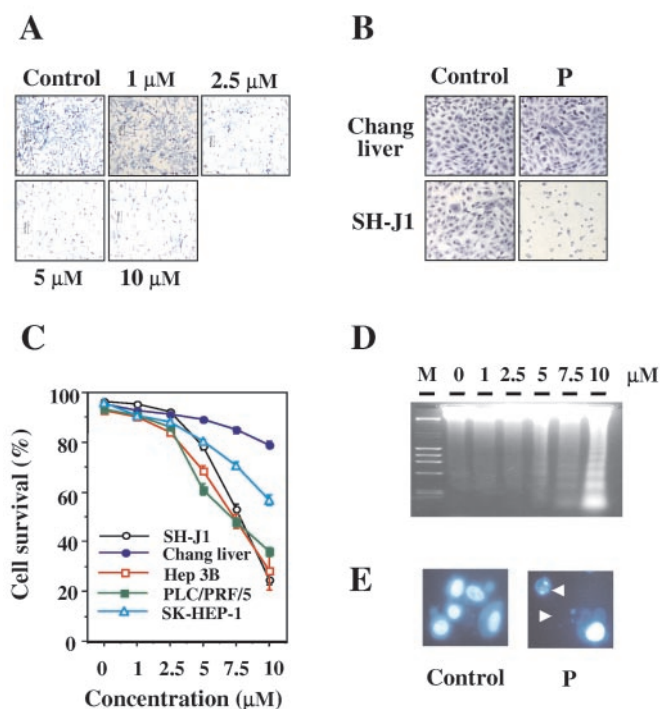


FIG. 1. Parthenolide-mediated growth inhibition and apoptotic cell death. *A*, growth inhibition of hepatoma cells after parthenolide treatment. SH-J1 cells were cultured on coverslips and treated with the indicated concentrations of parthenolide for 48 h. The cells were fixed with 4% paraformaldehyde in 0.1 M sodium phosphate buffer (pH 7.6) and stained with the Diff-Quick stain set. Cell numbers were photographically compared between cells treated with different concentrations of parthenolide. *B*, tumor cell-specific inhibition of cell growth. SH-J1 cells and Chang liver cells were cultured on coverslips and treated with 10 μM parthenolide for 48 h. The cells were fixed and stained with the Diff-Quick stain set. Cell numbers were photographically compared between SH-J1 cells and Chang liver cells. *C*, kinetics of cell death after drug treatment. Cells were treated continuously with the indicated concentrations of parthenolide for 48 h. SH-J1, Chang liver, Hep 3B, PLC/PRF/5, and SK-HEP-1 cells were harvested and then stained with trypan blue dye to determine cell viability. At least 200 cells were counted for each time point, and all counting was done in a blinded fashion. Each point represents the mean \pm S.E. of quadruplicate experiments (*P*, parthenolide). *D*, induction of internucleosomal DNA fragmentation by parthenolide. Cells were treated with various concentrations of parthenolide for 48 h. DNA was extracted and analyzed by 2% agarose gel electrophoresis in the presence of ethidium bromide (*M*, molecular mass standards). *E*, detection of apoptosis by Hoechst 33258 staining. Hepatoma cells were treated with vehicle (*Control*) or with 10 μM parthenolide (*P*) for 48 h. Cells were harvested, stained with Hoechst 33258, and viewed by fluorescence microscopy to determine the fraction of apoptotic cells (as described under "Materials and Methods"). Arrowheads indicate apoptotic nuclei of cells.

nolide effectively decreased cell numbers in a dose-dependent manner (Fig. 1A). To examine whether these cytotoxic effects of parthenolide are tumor cell-specific, SH-J1 cells and Chang liver cells (which were derived from normal liver tissue) were treated with 10 μM parthenolide for 48 h. Histocytological examination revealed that the nonmalignant Chang liver cells were resistant to parthenolide-mediated cell growth inhibition, as compared with SH-J1 cells. The cell numbers of Chang liver cells and SH-J1 cells are about 80 and 20% that of the untreated controls, respectively (Fig. 1B). The parthenolide-induced reduction of cell number may result from cell cycle inhibition or cytotoxic cell death. Thus, to measure quantitative cell death, SH-J1 cells, Chang liver cells, and ordinary hepatoma cells (Hep 3B, PLC/PRF/5, and SK-HEP-1) were cultured in 6-cm dishes and exposed to parthenolide at different concen-

trations (0–10 μM) for 48 h. The cells were harvested, and dead cells stained with trypan blue dye were counted. Parthenolide decreased SH-J1 cell survival in a dose-dependent manner, and the IC_{50} for cell survival was about 7.5 μM (Fig. 1C). The quantitation of cell survival of SH-J1 and Chang liver cells was consistent with the histocytological examination ($24.7 \pm 2.2\%$ versus $80.0 \pm 7.4\%$, $p < 0.01$). These results suggest that parthenolide exerts its cytotoxic effects in a tumor cell-specific manner. However, cytotoxic cell death was rarely detectable at lower concentrations (1–2.5 μM) of parthenolide. Hep 3B and PLC/PRF/5 cells were more susceptible to the drug-induced cell death than were SK-HEP-1 cells. To demonstrate whether parthenolide induces apoptotic cell death, DNA fragmentation was analyzed by gel electrophoresis. SH-J1 cells treated with parthenolide showed increased fragmentation of lower molecular weight DNAs at higher concentrations of parthenolide (between 5 and 10 μM) (Fig. 1D). Lower concentrations of parthenolide (0–2.5 μM) did not result in any DNA fragmentation. Cells with condensed or fragmented chromosomes and with membrane blebbing, both characteristics indicative of apoptotic morphologies, were examined by staining with Hoechst 33258 after treatment with parthenolide (5–10 μM) (Fig. 1E). These results indicate that parthenolide effectively induces apoptosis at the relatively higher concentrations but not at the lower concentrations.

Parthenolide Inhibits the Cell Cycle (G_2/M Arrest)—Lower concentrations of parthenolide seem to reduce cell number by cell cycle inhibition. This was supported by the previous report that parthenolide inhibited cell growth in a cytostatic fashion and that the effect was reversible at lower concentrations (10). Thus, we quantitatively determined the effect of parthenolide on cell proliferation at sublethal concentrations (1–3 μM). Using a thymidine uptake assay, DNA synthesis was significantly inhibited by 8–51% in cells treated with 1–3 μM parthenolide (Fig. 2A), which is consistent with a previous report (1). We next analyzed the impact of parthenolide on the cell cycle of SH-J1 cells. In asynchronous cells, parthenolide increased the fraction of cells in G_2/M from 15 to 30% compared with untreated control cells at 12 h of culture (Fig. 2B). Thus, we further studied the cell cycle inhibition in synchronized cells. For synchronization, SH-J1 cells were arrested in M phase with 0.5 $\mu\text{g/ml}$ nocodazole. Cells were then analyzed at 3-h interval after release from the M block in the presence or absence of parthenolide. Cells treated with parthenolide clearly showed delayed cell cycling (G_2/M arrest). In control cells, a normal cell cycle distribution appeared 12 h after release, whereas it appeared only after 36 h after release in cells treated with parthenolide.

Oxidative Stress Is Involved in Parthenolide-induced Apoptosis—Treatment of SH-J1 cells with 10 μM parthenolide resulted in $\sim 80\%$ apoptotic death within 48 h. Remarkably, in the presence of non-cytotoxic doses of general antioxidants, including NAC (800 μM), pyrrolidine dithiocarbamate (0.25 μM), and nordihydroguaiaretic acid (0.1 μM), the killing activity of parthenolide is effectively inhibited or abrogated (Fig. 3A). NAC was able to completely abrogate parthenolide-induced apoptosis ($95 \pm 5.5\%$ inhibition, $p < 0.01$). Vitamin E (200 μM) and vitamin C (200 μM) also effectively inhibited parthenolide-induced apoptosis by 40 ± 3.5 and by $18 \pm 2\%$, respectively ($p < 0.05$) (data not shown). Thus, the protection afforded by antioxidants against the induction of cell death by parthenolide suggests that free radicals may be involved in this phenomenon. To examine this possibility, we measured the levels of intracellular free radicals before and after exposure to parthenolide using the cell permeant dye DCFH-DA. Measurements of cellular fluorescence revealed that parthenolide generated a

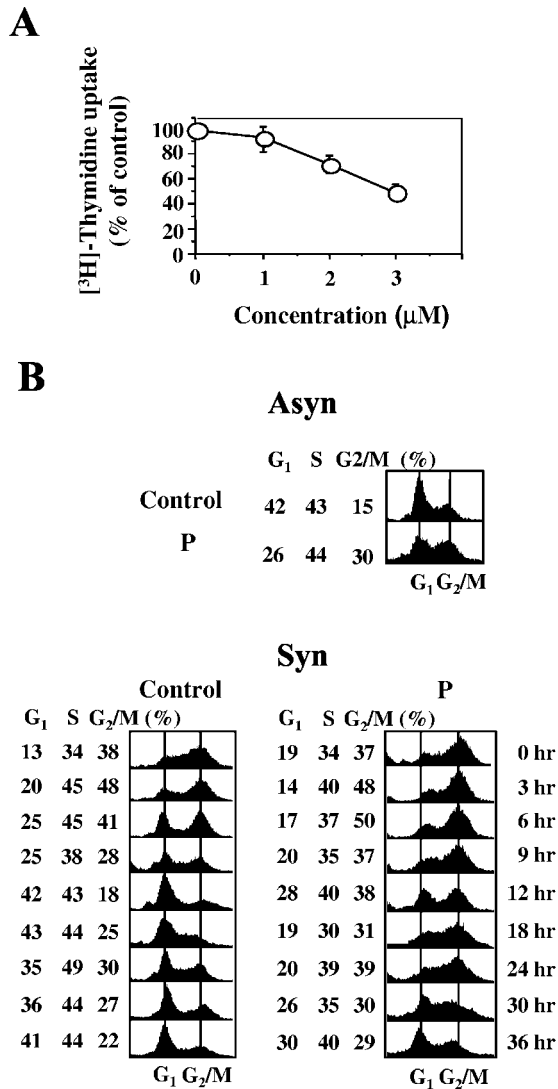


FIG. 2. Cell cycle inhibition by sublethal doses of parthenolide. A, effect of parthenolide on DNA synthesis. Exponentially growing cells were plated in 96-well microtiter plates at a density of 1×10^3 cells/well and treated with 1–3 μM parthenolide for 48 h. Twenty-four hours before harvest, 1 μCi of [^3H]thymidine was added to each well, and the incubation was continued for an additional 24 h. Cellular uptake of [^3H]thymidine was determined by liquid scintillation counting. Assays were performed in triplicate, and the experiment was repeated at least two times with similar results. Results are expressed as percent of untreated control, and each point represents the mean of quadruplicate experiments \pm S.E. B, effect of parthenolide treatment on cell cycle progression. Shown is cell cycle analysis in SH-J1 cells treated with 3 μM parthenolide (sublethal dose) for 48 h. In asynchronous cells, cell cycle distribution was performed 12 h after seeding using a FACSscan. For synchronization, SH-J1 cells were arrested in M phase by treatment with 0.5 $\mu\text{g}/\text{ml}$ nocodazole. Cells were analyzed at 3- or 6-h intervals after release from the M block. Data were analyzed as single-parameter frequency histograms in an SFIT model (P, parthenolide; Syn, synchronized; Asyn, asynchronous).

3-fold increase of intracellular ROS in SH-J1 cells. A noncytotoxic dose of NAC completely suppressed parthenolide-induced ROS generation (Fig. 3B). Reduction of $\Delta\Psi_m$ is believed to be mediated by ROS. An assay to detect these changes of $\Delta\Psi_m$ in mitochondrial function employs a fluorescent cation, JC-1, which emits a red color when sequestered in mitochondria of healthy cells but emits a green color when it is in the cytoplasmic compartment of apoptotic cells. Treatment of cells with 10 μM parthenolide for 48 h caused a disruption of $\Delta\Psi_m$, as

evidenced by a shift in the fluorescence of the probe JC-1, from $3.3 \pm 0.5\%$ in the right lower quadrant fluorescence fraction in control cells to $78.3 \pm 5.7\%$ in parthenolide-treated cells (Fig. 3C). The parthenolide-induced reduction in $\Delta\Psi_m$ was completely abrogated by NAC ($5.2 \pm 0.4\%$). The sum of these results suggests that parthenolide induces $\Delta\Psi_m$ dissipation in an antioxidant-sensitive pathway and indicates that parthenolide-mediated generation of ROS causes the reduction in $\Delta\Psi_m$.

Time Course of $\Delta\Psi_m$ Reduction, Cytochrome c Release, and Caspase Activation—The $\Delta\Psi_m$ disruption appears to be critical for the apoptosis cascade. To determine whether the loss of $\Delta\Psi_m$ precedes cytochrome c release, we analyzed the time course of $\Delta\Psi_m$ reduction and cytochrome c release. Flow cytometric measurements from 0 to 48 h after parthenolide treatment revealed that the percentage of cells with low $\Delta\Psi_m$ in the right lower quadrant began to increase 12 h after the treatment started and reached a maximum at the end of the experimental period, in a time-dependent manner (Fig. 4A). About 80% of the cells showed a collapsed $\Delta\Psi_m$ 48 h after treatment. The time course of cytochrome release analyzed by Western immunoblot revealed that cytosolic cytochrome c appeared 12 h after parthenolide treatment (Fig. 4B). Thus, our data suggest that the collapse in $\Delta\Psi_m$ correlates with mitochondrial cytochrome c release. Because caspase activation plays a central role in the induction of apoptosis (19), to understand the mechanism of parthenolide-induced apoptosis we examined its effect on the activation of initiator and effector caspases and cleavage of their substrate, PARP. The cleavage and/or the decreased level of the apoptotic substrate PARP and procaspase-7 (which is indicative of apoptotic cell death) were demonstrated along the time course, implying that cytochrome c release leads to apoptotic cell death through oxidative stress as previously described (20). Interestingly, parthenolide caused a decrease in the procaspase-7 level and its cleavage without changing the level of procaspases-3 or -6, implying that caspase-7 activation is the major effector pathway involved in parthenolide-induced apoptosis. Activation of initiator caspases-8 and -9 were observed in a time-dependent manner, as evidenced by decreased level or cleavage of their pro-caspases.

Endogenous GADD153 Induction by Parthenolide—To identify the gene(s) responsible for parthenolide-induced apoptosis, we screened genes known to be involved in drug-induced apoptosis through generation of ROS. We focused on *GADD153*, the growth arrest and DNA damage gene, because parthenolide triggered sudden *GADD153* mRNA overexpression during exposure to the drug (Fig. 5A). To determine the effect of parthenolide on the activation of the *GADD153* promoter, SH-J1 cells were transiently transfected with pGADD-LUC, which contains the hamster *GADD153* promoter coupled to the luciferase reporter gene. The transfected cells were exposed to 5 μM parthenolide for 48 h (Fig. 5B). The change in luciferase activity, expressed relative to the level in untreated control cells, indicated that parthenolide increased *GADD153* promoter activation maximally after 24 h of exposure, which preceded the increase of endogenous *GADD153* mRNA after 36 h of treatment with parthenolide. These results suggest that parthenolide transcriptionally regulates *GADD153* mRNA expression in SH-J1 cells. To further investigate the transcriptional regulation by parthenolide, the decline of *GADD153* mRNA levels in parthenolide-treated cells was examined after parthenolide withdrawal and/or the addition of an inhibitor of transcription, actinomycin D. Subconfluent SH-J1 cells were treated with 5 μM parthenolide for 48 h to bring about the accumulation of *GADD153* mRNA levels. Cells treated with parthenolide

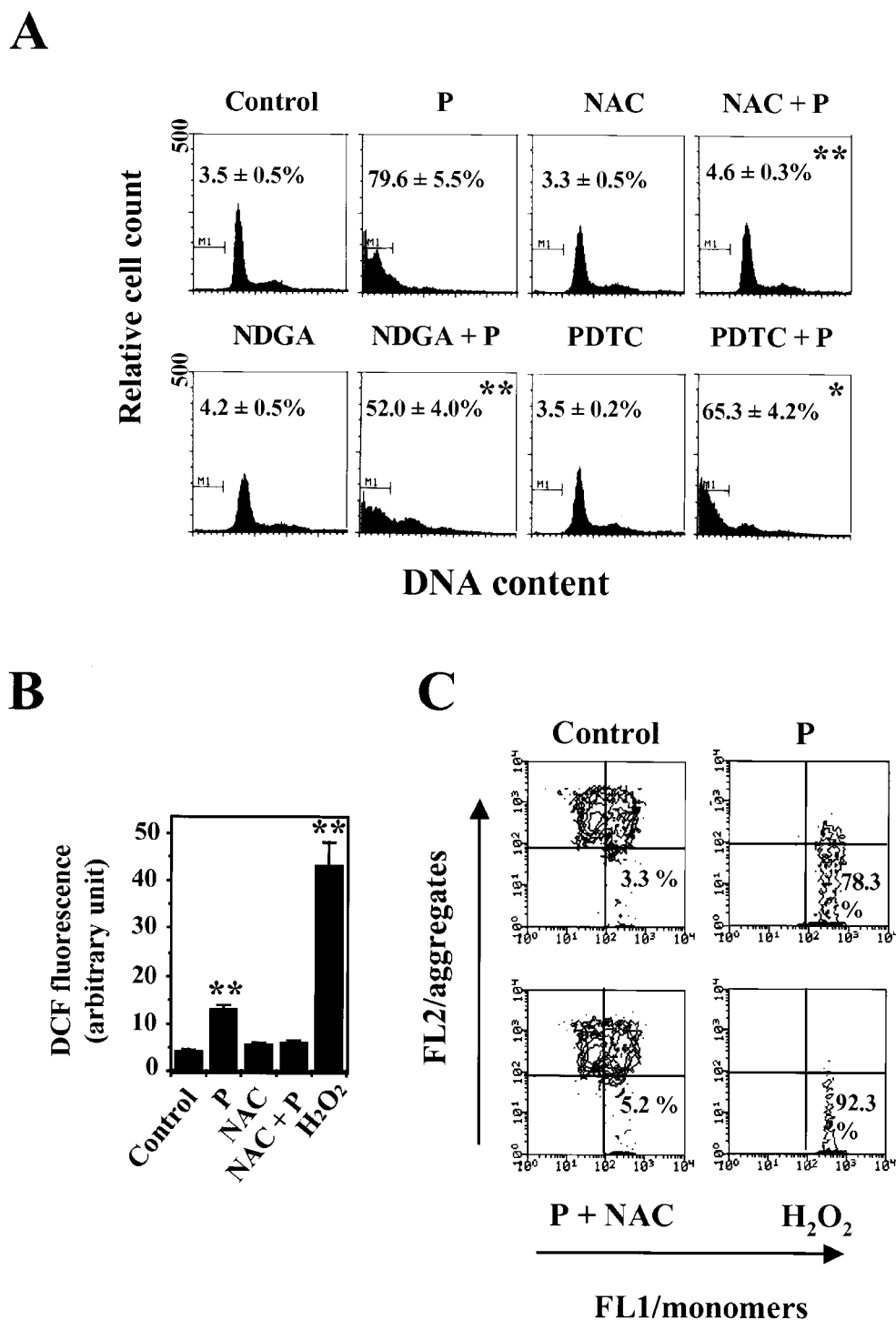


FIG. 3. Oxidative stress-mediated apoptotic cell execution after treatment with parthenolide. *A*, parthenolide-induced apoptosis is abrogated or inhibited by antioxidants. Shown is flow cytometric DNA analysis of SH-J1 cells; histograms were generated from analysis of propidium iodide-stained cells pretreated for 1 h with antioxidant (including NAC, NGDA, or pyrrolidine dithiocarbamate (PDTC)) and then for a further 48 h with 10 μ M parthenolide (*P*). The sub-G₁ fraction was estimated by gating hypodiploid cells in the DNA histogram using a C-30 program. Each value represents the mean \pm S.E. of duplicate assays in three independent experiments (*, $p < 0.05$; **, $p < 0.01$ compared with parthenolide treatment). *B*, ROS generation by parthenolide. The intracellular generation of ROS was measured using the oxidation-sensitive fluorescein DCFH-DA. Exponentially growing cells (2×10^5 /ml) were treated with or without 10 μ M parthenolide for 3 h or with 2 mM H₂O₂ for 1 h. The cells were collected and loaded with 50 μ M DCFH-DA for 30 min at 37 $^{\circ}$ C and then incubated for 4 h with antioxidant before loading with DCFH-DA. The fluorescence intensity of the cell suspension was measured using a fluorescence spectrophotometer with excitation at 488 nm and emission at 525 nm. Each value represents the mean \pm S.E. of duplicate assays in three independent experiments (**, $p < 0.01$ compared with control). *C*, ROS-mediated the reduction of $\Delta\Psi_m$ by parthenolide. $\Delta\Psi_m$ was detected by flow cytometric analysis using the probe JC-1. The relative intensity of green versus red fluorescence was plotted, and cells with a low $\Delta\Psi_m$ are found in the lower right quadrant. The values reported are the means of three independent experiments (*P*, parthenolide).

were then fed parthenolide-free medium to which actinomycin D (5 μ g/ml) or vehicle was added (21). At various times thereafter, relative mRNA levels were calculated by compar-

ing *GAPDH*-normalized values with the levels observed in cells at time 0 (Fig. 5C). Parthenolide sustained *GADD153* mRNA after treatment for 9 h in the cells. In the presence of

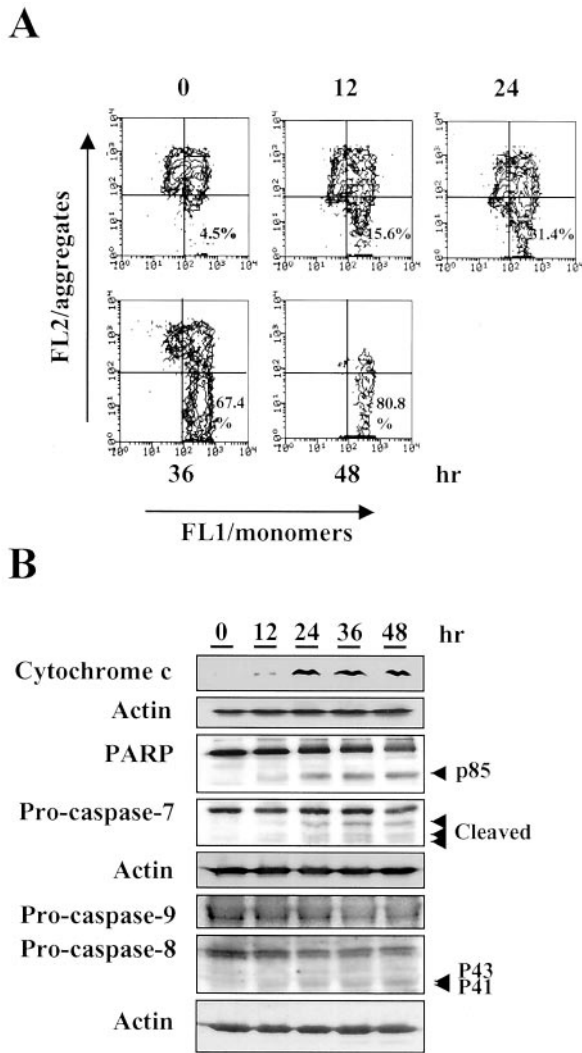


FIG. 4. Time courses of $\Delta\Psi_m$ reduction, cytochrome *c* release, and caspase activation. *A*, time course of changes in $\Delta\Psi_m$ dissipation. SH-J1 cells were treated with 10 μM parthenolide, and $\Delta\Psi_m$ was detected by flow cytometric analysis using the *J* aggregate-forming dye JC-1. The relative intensity of green versus red fluorescence was plotted and reveals the range of lower fluorescence representing the loss of $\Delta\Psi_m$ in the lower right quadrant. This experiment was repeated three times with similar results. *B*, time course of changes in cytochrome *c* release and caspase activation. Cells were treated with 10 μM parthenolide for the indicated times. The S-100 fraction of cytosolic proteins (30 μg) were separated by 15% SDS-PAGE. The blot was probed with a monoclonal antibody to cytochrome *c* (1:2000). Thirty μg of protein/lane isolated from cell lysates were separated by 15% SDS-PAGE. Immunodetection of PARP, caspases-7, -8, and -9 was performed by specific antibodies as detailed under "Materials and Methods" and was visualized by enhanced chemiluminescence.

actinomycin D, parthenolide decreased the *GADD153* mRNA levels as if parthenolide had been removed from the culture medium. These results imply that parthenolide regulates *GADD153* mRNA levels transcriptionally in SH-J1 cells, in accordance with results from the *in vitro* transfection experiment.

Glutathione-sensitive *GADD153* Overexpression during Parthenolide-induced Apoptosis—Parthenolide-induced apoptosis was completely blocked by NAC, a glutathione precursor, but other general antioxidants, including pyrrolidine dithiocarbamate, nordihydroguaiaretic acid, vitamin C, and vitamin E, did not block this apoptosis to the same extent, suggesting that the induction of oxidative stress by parthe-

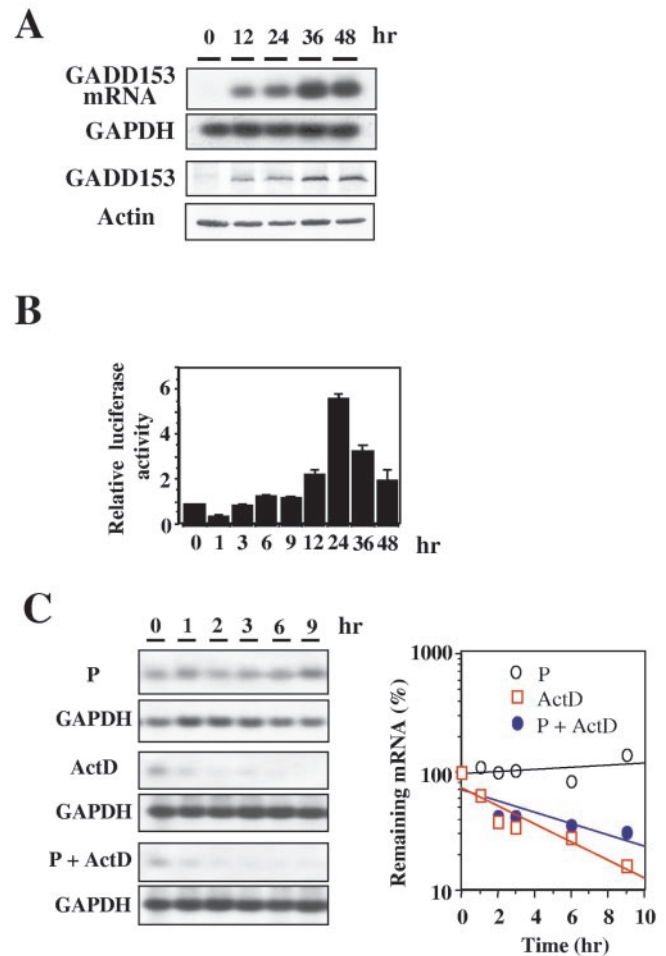
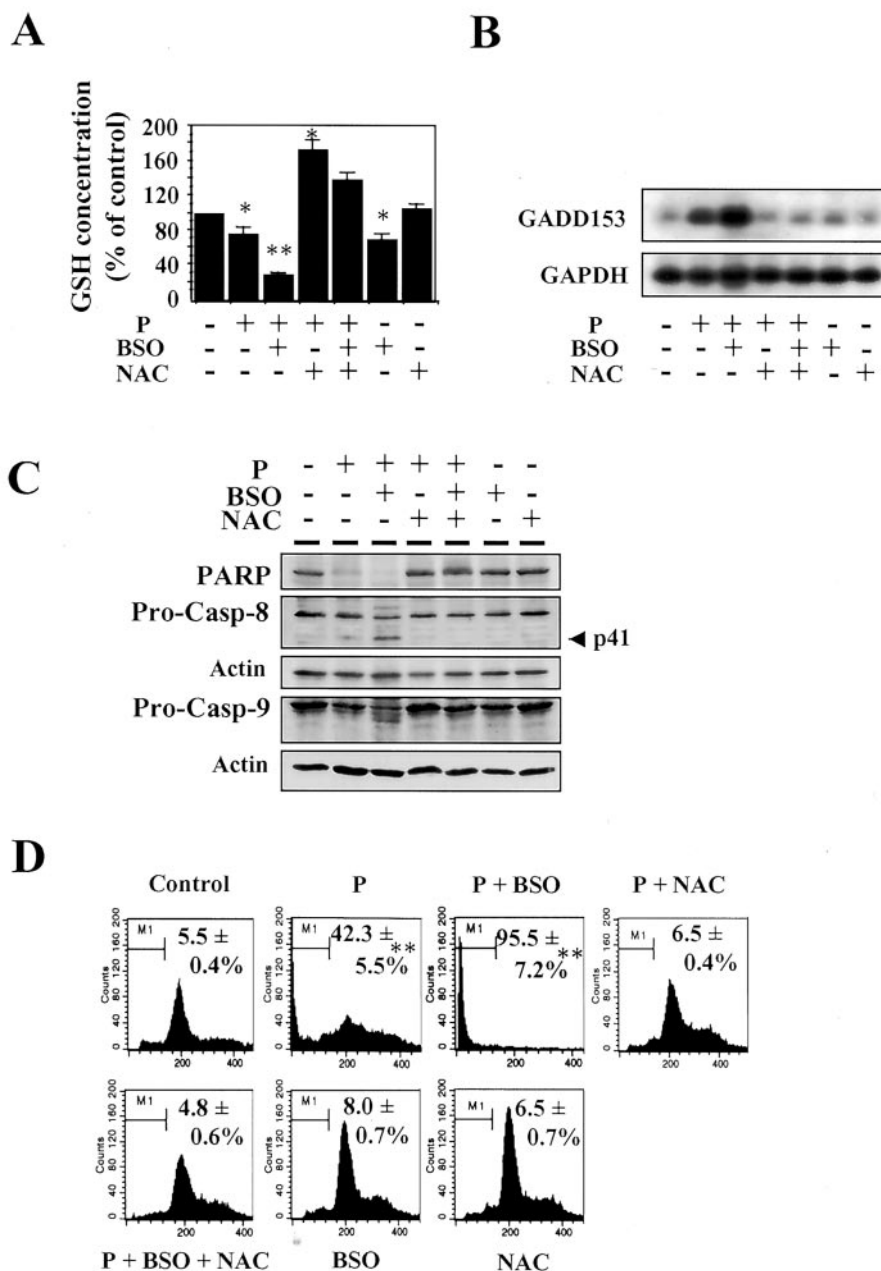


FIG. 5. Endogenous *GADD153* mRNA overexpression induced by parthenolide. *A*, endogenous *GADD153* mRNA overexpression induced by parthenolide. Total RNA extracts from SH-J1 cells treated with 5 μM parthenolide were fractionated by electrophoresis on 1% agarose gels containing formaldehyde and then transferred to membranes. Blots were hybridized overnight with 2×10^6 cpm/ml *GADD153* cDNA probe labeled with [^{32}P]dCTP by random-priming, washed, then exposed to X-Omat AR film at -70°C . The blot was stripped and subsequently rehybridized with a probe for *GAPDH* cDNA as a loading control (*lower*). *B*, luciferase activity measured in SH-J1 cells transiently transfected with pGADD-LUC. The cells were treated with 5 μM parthenolide for the indicated time-intervals. The values are the means \pm S.E. of duplicate assays in two independent experiments. *C*, the decay of *GADD153* transcript in Hep 3B cells or SK-HEP-1 cells. The cells were treated with 5 μM parthenolide for 48 h and then cultured in parthenolide-free medium to which actinomycin D (*ActD*, 5 $\mu\text{g}/\text{ml}$) or vehicle with or without 5 μM parthenolide (*P*) was added. Total RNA was extracted from the three sets at subsequent time points (*left*). Autoradiograms were read using densitometric scanning and were normalized against *GAPDH* mRNA levels (*right*).

nolide may be related to glutathione depletion. Thus, we measured the cellular glutathione level during parthenolide-induced apoptosis. Parthenolide exposure resulted in a time-dependent decrease in cellular glutathione, which was about 75% that of the control level within 48 h (Fig. 6A). NAC (800 μM) abrogated the parthenolide-mediated glutathione depletion but increased the cellular glutathione level ($171\% \pm 15.2\%$, $p < 0.05$), implying that parthenolide-induced glutathione depletion activates the glutathione rescue system for compensation, whereas pretreatment with BSO (1 mM) synergistically enhanced parthenolide-mediated glutathione depletion ($28.7 \pm 1.2\%$, $p < 0.01$). BSO-mediated glutathione depletion was recovered by the addition of NAC ($137.7 \pm$

FIG. 6. Glutathione depletion correlates with *GADD153* overexpression.

A, reduced levels of cellular glutathione in SH-J1 cells treated either with 10 μ M parthenolide (*P*) alone or in combination with NAC (800 μ M) and/or BSO (1 mM) for 48 h. Cellular glutathione levels were measured using a colorimetric assay kit as described under "Materials and Methods" (*, $p < 0.05$; **, $p < 0.01$). **B**, total RNA extracts from SH-J1 cells treated either with parthenolide (*P*, 10 μ M) alone or in combination with NAC (800 μ M) and/or BSO (1 mM) for 48 h were fractionated by electrophoresis on 1% agarose gels containing formaldehyde and then transferred to membranes. Northern blot analysis was performed. The blot was stripped and subsequently rehybridized with a probe for *GAPDH* cDNA as a loading control (*lower*). **C**, activation of caspases in SH-J1 cells treated with 10 μ M parthenolide (*P*) in the presence or absence of NAC and/or BSO. Thirty μ g of protein/lane isolated from cell lysates were separated by 15% SDS-PAGE. Immunodetection of PARP, caspase-8, and caspase-9 was performed using antibodies listed under "Materials and Methods" and by enhanced chemiluminescence. **D**, quantification of apoptotic fractions was performed using a FACScan as described under "Material and Methods." SH-J1 cells were treated either with 10 μ M parthenolide (*P*) alone or in combination with NAC (800 μ M) and/or BSO (1 mM) for 48 h. The sub- G_1 fraction was estimated by gating hypodiploid cells in the histogram using a C-30 program. DNA contents are plotted on the linear abscissa (M_1 , apoptotic fraction). Each value represents the mean of triplicate experiments \pm S.E. (**, $p < 0.01$ compared with control).



10.2%). Subsequently we examined whether the cellular glutathione level is related to *GADD153* mRNA overexpression. Interestingly, the cellular glutathione level was inversely related to *GADD153* overexpression (Fig. 6B), which suggested that parthenolide-mediated glutathione depletion quantitatively triggered *GADD153* overexpression. We further determined whether the glutathione-sensitive induction of *GADD153* is involved in apoptotic cell execution through activation of initiator and effector caspases. After treatment with 10 μ M parthenolide alone, the level of PARP was decreased through cleavage. Furthermore, BSO enhanced the parthenolide-mediated cleavage of PARP, whereas NAC completely prevented the cleavage of PARP (Fig. 6C). These findings are consistent with the parthenolide-induced apoptotic cell execution. Similarly, the decreased level and appearance of cleaved procaspases-9 or -8 was observed. In addition, using flow cytometry we quantified the percentage of the apoptotic cell fraction in sub- G_1 DNA content. 5 μ M parthenolide caused 42.3% (\pm 5.5%) apoptotic cell death within 48 h (Fig. 6D). NAC completely prevented parthenolide-

induced apoptosis (6.5 \pm 0.4%), whereas BSO pretreatment synergistically enhanced parthenolide-induced apoptosis (95.5 \pm 7.2%, $p < 0.01$). In addition, NAC overcame the enhancement of parthenolide-induced apoptosis by BSO (4.8 \pm 0.6%). These results are consistent with the glutathione depletion-mediated overexpression of *GADD153*. Therefore, NAC treatment seems to completely prevent the parthenolide-mediated glutathione depletion and the *GADD153* overexpression, which in turn almost blocked apoptotic cell death. Thus, glutathione depletion seems to be in the highest upstream pathway of parthenolide-mediated *GADD153* overexpression and apoptotic cell death.

Effect of Modulation of *GADD153* Expression on Apoptosis—We next examined whether *GADD153* induction was related to parthenolide-induced apoptosis. We established two stable cell lines that overexpressed *GADD153* (J1-G1 and J1-G3). These cells grew slowly without any phenotypic differences but were readily susceptible to parthenolide-induced apoptosis compared with vector-only transfected controls (J1-C1 and J1-C3) (Fig. 7A). A 2-fold increase of apoptosis was

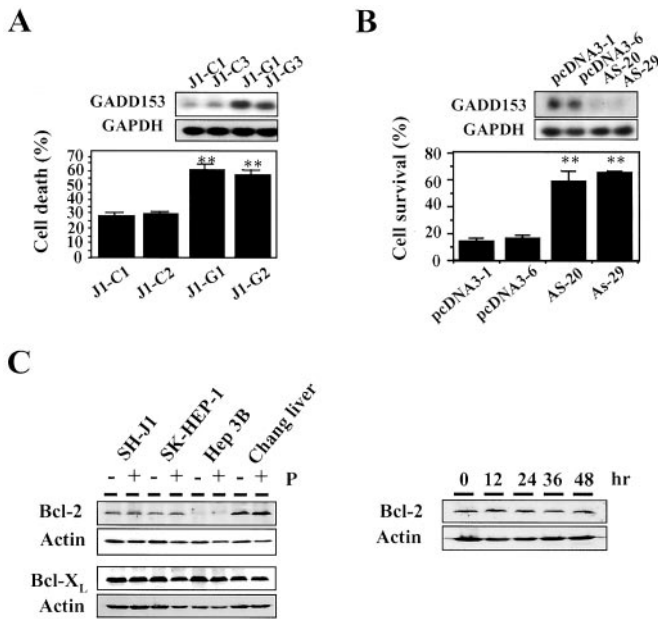


FIG. 7. Effects of modulated expression of *GADD153* on apoptotic cell death. A, the mRNA expression of *GADD153* in stably transfected cells (J1-G1 and J1-G2) compared with vector control cells (J1-C1 and J1-C3) (upper panel). Total RNA extracts from the transfectants were fractionated by electrophoresis on 1% agarose gels containing formaldehyde and then transferred to membranes. Northern blot analysis was performed as described under "Materials and Methods." Shown are the effects of 5 μ M parthenolide treatment for 48 h on cell death of stably *GADD153*-transfected SH-J1 cells. Apoptotic cell death was determined by Hoechst 33258 staining (lower panel), and experiments were performed in duplicate and repeated twice with similar results. Vertical bars represent the means \pm S.E. of quadruplicate experiments (**, $p < 0.01$). B, The mRNA expression of *GADD153* in stably transfected cells with *GADD153* antisense (AS-20 and AS-29) compared with vector control cells (pcDNA3-1 and pcDNA3-6) (upper panel). SH-J1 cells transfected with *GADD153* cDNA antisense were treated with 10 μ M parthenolide for 48 h. Apoptotic cell death was determined by Hoechst 33258 staining (lower panel), and experiments were performed in duplicate and repeated twice with similar results. Vertical bars represent the means \pm S.E. of quadruplicate experiments (**, $p < 0.01$). C, hepatoma cells (SH-J1, SK-HEP-1, Hep 3B, and Chang liver) were treated with (+) or without (-) 10 μ M parthenolide (P) for 48 h. Thirty μ g of protein/lane isolated from cell lysates were separated by 15% SDS-PAGE. Immunodetection of Bcl-2 or Bcl-X_L was performed using mouse anti-Bcl-2 monoclonal antibody (Ab-1) or mouse anti-Bcl-X_L monoclonal antibody (H-5) and enhanced chemiluminescence (left). Time course analysis of Bcl-2 protein expression in SH-J1 cells in the period of parthenolide treatment in SH-J1 cells is shown on the right.

induced by 5 μ M parthenolide in the stably *GADD153*-transfected cells compared with the vector-only transfectants (59.6 ± 5.2 and $55.5 \pm 4.0\%$ versus 27.2 ± 3.2 and $29.3 \pm 2.1\%$, $p < 0.01$). Thus, the induction of *GADD153* seems to sensitize the cells to undergo apoptosis. To support this hypothesis, we used transfection of an antisense expression plasmid of *GADD153*. During parthenolide-induced apoptosis, *GADD153* mRNA overexpression was inhibited in SH-J1 cells transfected with the antisense *GADD153* cDNA (J1-AS20 and J1-AS29). J1-AS20 and J1-AS29 cells were significantly resistant to 10 μ M parthenolide, e.g. about 59.2 ± 7.3 and $65.1 \pm 1.8\%$ of *GADD153* antisense transfectants survived ($p < 0.01$) compared with 13.9 ± 2.5 and $16.2 \pm 3.0\%$ of vector control cells (pcDNA3-1 and pcDNA3-6) (Fig. 7B), implying that inhibition of *GADD153* mRNA expression correlates well with cell survival in hepatoma cells. These results suggest that *GADD153* overexpression after parthenolide treatment may play a role in sensitizing the cancer cells to drug-induced apoptotic cell execution.

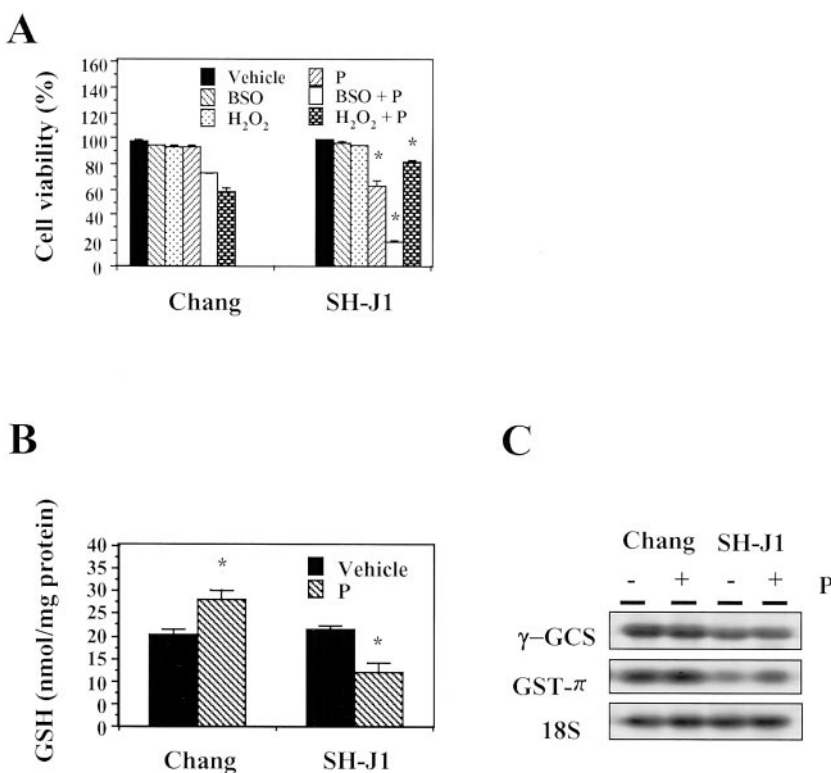
Overexpression of *GADD153* sensitized cells to endoplasmic reticulum stress through the down-regulation of Bcl-2 expression. This down-regulation of Bcl-2 expression enhanced oxidant injuries, e.g. depletion of cellular glutathione and exaggerated the production of ROS (22). Thus, we determined the effect of parthenolide on Bcl-2 or Bcl-X_L expression in hepatoma cells. In the present study, Hep 3B cells are defective in Bcl-2 expression, whereas SH-J1, SK-HEP-1, and Chang liver cells expressed Bcl-2 protein as we previously observed (18). Treatment with 10 μ M parthenolide for 48 h did not elicit significant changes of Bcl-2 or Bcl-X_L expression levels in hepatoma cells (Fig. 7C). Time course analysis also revealed that Bcl-2 protein expression did not change or was only slightly increased in the early period of parthenolide treatment in SH-J1 cells (Fig. 7C, right panel).

Parthenolide-mediated Tumor Cell-specific Oxidative Stress—To determine whether the increase in oxidative stress is caused by increased production of ROS or by increased consumption of GSH during detoxification of parthenolide, we treated SH-J1 cells with either a nontoxic dose of BSO (1 mM) or with H₂O₂ (0.3 mM) alone or in combination with parthenolide (5 μ M). Cell viability was determined and compared with those of Chang liver cells. BSO significantly enhanced parthenolide-induced cell death and subsequently decreased viability of SH-J1 cells compared with Chang liver cells (19.3 ± 1.6 versus $72.2 \pm 0.7\%$). In contrast, H₂O₂ increased cell viability of SH-J1 cells compared with Chang liver cells (81.5 ± 2.1 versus $58.9 \pm 1.6\%$) (Fig. 8A). These results imply that GSH depletion rather than ROS generation plays a major contributing role in parthenolide-mediated oxidative stress. Next, we needed to explain the difference in the sensitivity to parthenolide between tumor cells and nontumor cells. We measured cellular GSH content before and after 48 h of parthenolide treatment (10 μ M). The GSH content of both types of cells were similar (~ 20 nmol/mg of protein) before the treatment, which is consistent with a previous report of hepatoma cells (23). However, parthenolide treatment significantly decreased the cellular GSH content in SH-J1 cells, whereas it increased the cellular GSH content in Chang liver cells (Fig. 8B). These findings suggest that the tumor cells are more sensitive to parthenolide, i.e. they experience a greater decrease in cellular GSH content in response to parthenolide. To support this hypothesis, we checked the expression of γ -glutamylcysteine synthetase, which is the rate-limiting enzyme in the synthesis of GSH (24), and of the multifunctional detoxification enzyme glutathione S-transferase π (GST- π), which plays a role in determining sensitivity to some drugs (25). Constitutive expression levels of γ -glutamylcysteine synthetase mRNA were slightly different in the two cell lines, although the cellular GSH levels were similar. Intriguingly, the basal expression of GST- π mRNA was much less (25%) in the tumor cells than in the nontumor cells. Parthenolide induced the overexpression of GST- π mRNA in SH-J1 cells, but it was still much less (50%) than that found in Chang liver cells.

DISCUSSION

Regarding the potential use of parthenolide and related compounds as chemotherapeutic agents, evidence is required that the agent(s) has a pronounced differential effect on tumor cells of any type compared with normal cells. Interestingly, parthenolide showed tumor cell-specific effects with respect to cytotoxic cell injuries. Cytotoxic events may be irreversible and can result from immediate effects (such as major disruption of cell membranes) or from delayed effects (such as triggering of apoptosis or interference with cell division). Our study revealed that parthenolide effectively induces apoptosis in hepatoma

FIG. 8. Effect of parthenolide on tumor cell-specific oxidative stress. A, Chang liver and SH-J1 cells were treated with either 1 mM BSO or 0.3 mM H₂O₂ alone or in combination with 5 μ M parthenolide (P) for 48 h. Cell viability was determined using the trypan blue dye exclusion method. Vertical bars represent the means \pm S.E. of duplicate assays in two independent experiments (*, significantly different from Chang liver cells treated with the same reagents at $p < 0.01$). B, SH-J1 and Chang liver cells were treated with 10 μ M parthenolide or vehicle for 48 h. Cellular glutathione levels were measured using a colorimetric assay kit as described under "Materials and Methods." Vertical bars represent the means \pm S.E. of duplicate assays in two independent experiments (*, significantly different from cells treated with vehicle at $p < 0.01$). C, total RNA extracts from cells treated with 5 μ M parthenolide (+) or vehicle (-) were fractionated by electrophoresis on 1% agarose gels containing formaldehyde, and then transferred to membranes. Blots were hybridized overnight with γ -CGS light subunit cDNA or *GST- π* cDNA probe. The blot was stripped and subsequently rehybridized with a probe for 18 S cDNA as a loading control.



cells. Because parthenolide was reported to inhibit cell growth in a cytostatic fashion, this study also showed that a sublethal dose of parthenolide induces G₂/M arrest in cancer cells as other apoptosis-inducing anticancer drugs frequently induce G₂/M arrest (26). In contrast, human sarcomatous cholangiocarcinoma cells treated with parthenolide showed G₁ arrest (data not shown). Thus, inhibition of the cell cycle phase seems to be cell-specific, although the exact molecular mechanism remains unknown.

NF- κ B is a heterodimeric transcription factor that is usually sequestered in the cytoplasm by I κ B proteins (27). In most cell types, NF- κ B induces the expression of proinflammatory and anti-apoptogenic genes and protects them against tumor necrosis factor, chemotherapeutic agents, and/or radiation (27–29). Recently, NF- κ B was reported to repress *GADD153* activation, and parthenolide was shown to sensitize breast cancer cells to endoplasmic reticulum stress (30). Furthermore, parthenolide and I κ B α increase paclitaxel-induced apoptosis by inhibiting a distinct NF- κ B-regulated cell survival pathway (31). Parthenolide is known as an inhibitor of NF- κ B via targeting of the I κ B kinase complex (7), and it subsequently prevents expression of NF- κ B-induced anti-apoptotic genes, including *c-IAP1*, *c-IAP-2*, *TRAF1*, *TRAF2*, *Bfl-1/A1*, *Bcl-XL*, and manganese superoxide dismutase (32–36). Thus, inhibition of NF- κ B activation by I κ B or by drugs with anti-NF- κ B properties can enhance anti-cancer drug-induced apoptosis. In contrast, this study demonstrated that parthenolide alone induces apoptotic cell execution in hepatoma cells in which the constitutive activation of NF- κ B was barely detectable. Furthermore, this drug-induced apoptosis is effectively abrogated or inhibited by antioxidants. Thus, we assume that another pathway such as oxidative stress might be involved in the parthenolide-induced apoptosis. We further observed that parthenolide generates ROS and dissipates $\Delta\Psi_m$ and that the oxidative stress leads to caspase activation. One major caspase activation cascade is triggered by cytochrome *c* release from the intermembrane space of mitochondria. Upon receiving an apoptotic stimulus

such as oxidative stress or a perturbation in mitochondrial respiration, the loss of mitochondrial membrane potential and opening of the mitochondrial outer membrane channel (the so-called permeability transition) allows cytochrome *c* release to the cytosol. Cytochrome *c* binds to Apaf-1 in a 2:1 ratio, forming an oligomeric Apaf-1-cytochrome *c* complex (apoptosome) in the presence of dATP or ATP (37). This oligomerized Apaf-1-cytochrome *c* complex then recruits the initiator caspase of this pathway, procaspase-9, and induces its autoactivation (37, 38). Caspase-9 in turn activates downstream caspases including caspases-3, -6, and -7 (38, 39). Parthenolide-induced apoptosis and its inhibition by antioxidants correlate with ROS generation and the loss of $\Delta\Psi_m$. Thus, we examined the time course of cytochrome *c* release and caspase activations according to the change of $\Delta\Psi_m$ after treatment with parthenolide. As expected, the reduction of $\Delta\Psi_m$ and simultaneous cytochrome *c* release were detected during the time course. The effector caspase-7 was activated during parthenolide-induced apoptosis in a time-dependent manner. However, caspases-3 and -6 were not activated (data not shown). Parthenolide activates caspase-8 in addition to oxidative stress-mediated caspase-9 activation. Caspase-8 activation may also be caused by the activated mitochondrial pathway of apoptosis because antioxidants completely block the parthenolide-induced apoptosis. Apoptogenic proteins released from mitochondria undergoing permeability transition, such as apoptosis-inducing factor, have been shown to induce cleavage of caspase-8, possibly by a direct effect on caspase-8, whereas cytochrome *c* did not cleave caspase-8 (40).

GADD153 is a gene that is strongly transcriptionally activated by various types of stress and by chemotherapeutic drugs. Induction of the *GADD153* gene by anti-cancer agents has been shown to be associated with cell injury/apoptosis (21, 41, 42) and to be attenuated in drug-resistant cells (43). Furthermore, introduction of *GADD153* into cancer cells increased their sensitivity to anticancer agents (44). Thus, *GADD153*

seems to be an important target gene for apoptotic cell death induced by anticancer agents. *GADD153* is known to be an AP-1-regulated gene that plays a critical role in the AP-1-associated signal transduction pathway(s) leading to apoptosis after oxidative stress (45). *GADD153* overexpression was detected by Northern blot in a time-dependent manner. It seems unclear whether parthenolide has a direct effect on *GADD153* or whether changes in *GADD153* expression occur farther downstream of the immediate effects of parthenolide. *GADD153* was reported to be a downstream gene of the immediate early response gene NF- κ B. NF- κ B represses *GADD153* promoter activity (30). Parthenolide-induced apoptotic cell death was completely blocked by NAC, but other general antioxidants including pyrrolidine dithiocarbamate and nordihydroguaiaretic acid did not seem to have much effect on this apoptosis, suggesting that parthenolide-mediated oxidative stress may be related to glutathione depletion. This hypothesis is supported by a recent report that parthenolide contains an α,β -unsaturated lactone that is capable of participating in a Michael addition with compounds containing an -SH group. Thus, it could conjugate with the antioxidant glutathione, levels of which are reduced in treated organisms (46). Accordingly, our study demonstrates that parthenolide decreases the cellular glutathione level and that parthenolide-mediated glutathione depletion is modulated by BSO or NAC. Furthermore, the modulation of oxidative stress changed *GADD153* induction, *i.e.* a decreased glutathione level inversely correlates with *GADD153* mRNA levels, caspase activation, and subsequent apoptotic cell death. Thus, glutathione depletion may be in the upstream pathway of the oxidative stress-mediated apoptosis after parthenolide treatment. These results are supported by a previous report (47) wherein NAC completely abrogated the *GADD153* overexpression induced by cadmium chloride, an oxidative stress-inducing agent, by interacting with and decreasing the levels of cellular glutathione. The cleavage of PARP was indicative of apoptotic cell death in parthenolide-treated cells, and this cleavage was enhanced by BSO and completely abrogated by NAC, implying that glutathione depletion is critical in triggering apoptotic cell execution. Activation of the initiator caspases-8, and -9 was similarly enhanced or inhibited by BSO or NAC, respectively.

In this study, ectopic *GADD153* overexpression-sensitized cells readily underwent apoptosis, whereas inhibition of *GADD153* overexpression correlated with drug resistance. Previously, parthenolide has been found to inhibit protein-tyrosine kinases (8) and protein kinase C (49). Protein kinase inhibitors have also been shown to cause apoptosis, although their exact mechanism is still unclear (50), and such inhibitors represent a promising new class of therapeutic agents against cancer. However, pretreatment of SH-J1 cells with a nonspecific inhibitor of protein kinase C (H7) or with a tyrosine kinase inhibitor (genestein) had no effect on the basal expression of *GADD153* mRNA and had a slight modulation of parthenolide-induced *GADD153* mRNA levels (data not shown), which implies that the parthenolide-induced expression of *GADD153* is independent of protein kinase c or tyrosine kinase. These findings are consistent with the effects of protein kinase inhibitor and genestein on methyl methanesulfonate-induced *GADD153* mRNA expression in HeLa cells (47). In addition, the *GADD153*-transfected cells had an increased sensitivity to parthenolide-mediated cytotoxicity that was associated with cell death. Other groups have previously reported that induction of *GADD153* correlates with the onset of apoptosis (51, 52). In contrast, it has been recently reported that *GADD153*-mediated down-regulation of Bcl-2 expression enhanced oxidant

injuries, *e.g.* depletion of cellular glutathione and exaggerated production of ROS (22). However, parthenolide did not change any detectable Bcl-2 expression either in parthenolide-susceptible SH-J1 and SK-HEP-1 cells or in the resistant Chang liver cells. Considering that some hepatoma cells are defective for Bcl-2 expression and that parthenolide does not alter the expression level of Bcl-2 even in Bcl-2-positive hepatoma cells, another alternative pathway to *GADD153*-mediated down-regulation of Bcl-2 expression seems to play a causative role in this drug-induced apoptosis in hepatoma cells. Furthermore, parthenolide does not change the expression level of Bcl-X_L in hepatoma cells.

Sesquiterpene lactones possessing an α -methylene γ -lactone functionality are electrophilic agents and are, thus, apt to react with biological nucleophiles such as the sulfhydryl group of GSH, proteins, and parts of DNA (53). Previously, reduction of cellular GSH levels *in vitro* and *in vivo* has been reported for tumor cells exposed to sesquiterpene lactones (54, 55). Parthenolide, furthermore, also possesses an epoxide moiety, which is a second site for potential nucleophilic attack by an amino acid side chain. Accordingly, the present study showed that the parthenolide-mediated oxidative stress mainly resulted from the GSH depletion and that the tumor cell sensitivity to this sesquiterpene lactone seemed to correlate with glutathione metabolism. The critical reaction for GSH synthesis is catalyzed by γ -glutamylcysteine synthetase and by glutathione synthetase (56, 24). The cellular level of GSH is also controlled by glutathione peroxidase and by GST (24). Particularly, GST- π , a major cytoplasmic isoform of GSTs, is the most prevalent isoform expressed in tumor cells and in neoplastic tissues (57) and frequently plays a role in determining the sensitivity to some drugs (58). The expression level of γ -glutamylcysteine synthetase did not seem to be proportional to the cellular GST content between these two cell lines, even in drug-treated cells. However, untreated tumor cells expressed markedly less GST- π mRNA than did nontumor cells. GST- π forms a drug-GSH adduct, which is in turn transported outside the tumor cells (48), and this efflux activity is elevated in cells resistant to the drug. Thus, the abundant expression of GST- π may result in the acquisition of drug resistance in Chang liver cells. Furthermore, parthenolide induced the overexpression of GST- π mRNA only in tumor cells, which seems to be relevant to the parthenolide-mediated decrease of cellular GSH concentration. Considering that the tumor cell sensitivity to parthenolide is potentiated by lowering GSH levels by treatment with BSO, GSH homeostasis maintained by an interaction between GST- π and γ -glutamylcysteine synthetase may be critical for parthenolide-induced apoptotic cell execution in the parthenolide-sensitive hepatoma cells.

In summary, it is not currently known how overexpression of the *GADD153* gene connects to the downstream signal transduction pathway that leads to apoptosis and cell growth arrest. However, our data reveal that parthenolide triggers apoptotic cell death through oxidative stress, during which *GADD153* is overexpressed and sensitizes the tumor cells to apoptosis. Apoptotic cell death and cell growth inhibition appear to contribute to the anticancer effects of parthenolide, and these anticancer effects may be further modulated by pro- or anti-oxidants in a glutathione-sensitive manner.

Acknowledgement—We are grateful to Dr. Nikki J. Holbrook for providing the pGADD-LUC and the *GADD153* expression vector.

REFERENCES

1. Johnson, E. S., Kadam, N. P., Hylands, D. M., and Hylands, P. J. (1985) *Br. Med. J.* **31**, 569–573
2. Biggs, M. J., Johnson, E. S., Persaud, N. P., and Ratcliffe, D. M. (1982) *Lancet* **2**, 776

3. Hall, I. H., Lee, K. H., Starnes, C. O., Sumida, Y., Wu, R. Y., Waddell, T. G., Cochran, J. W., and Gerhart, K. G. (1979) *J. Pharmacol. Sci.* **68**, 537–542
4. Douros, J., and Suffness, M. (1978) *Cancer Chemother. Pharmacol.* **1**, 91–100
5. Lee, K. H., Hall, I. H., Mar, E. C., Starnes, C. O., ElGebaly, S. A., Waddell, T. G., Hadgraft, R. I., Ruffner, C. G., and Weidner, I. (1977) *Science* **196**, 533–536
6. Bork, P. M., Schmitz, M. L., Kuhnt, M., Escher, C., and Heinrich, M. (1997) *FEBS Lett.* **402**, 85–90
7. Hehner, S. P., Hofmann, T. G., Droge, W., and Schmitz, M. L. (1999) *J. Immunol.* **163**, 5617–5623
8. Hwang, D., Fischer, N. H., Jang, B. C., Tak, H., Kim, J. K., and Lee, W. (1996) *Biochem. Biophys. Res. Commun.* **226**, 810–818
9. Fukuda, K., Hibiya, Y., Mutoh, M., Ohno, Y., Yamashita, K., Akao, S., and Fujiwara, H. (2000) *Biochem. Pharmacol.* **60**, 595–600
10. Ross, J. J., Arnason, J. T., and Birnboim, H. C. (1999) *Planta Med.* **65**, 126–129
11. Haratake, J., and Horie, A. (1991) *Cancer* **68**, 93–97
12. Maeda, T., Adachi, E., Kajiyama, K., Takenaka, K., Sugimachi, K., and Tsuneyoshi, M. (1996) *Cancer* **77**, 51–57
13. Nakajima, T., Tajima, Y., Sugano, I., Nagao, K., Kondo, Y., and Wada, K. (1993) *Cancer* **72**, 1872–1877
14. Kim, D. G., Park, S. Y., Kim, H., Chun, Y. H., Moon, W. S., and Park, S. H. (2002) *Cancer Genet. Cytogenet.* **132**, 120–124
15. Kim, D. G., Jo, B. H., You, K. R., and Ahn, D. S. (1996) *Cancer Lett.* **107**, 149–159
16. You, K. R., Wen, J., Lee, S. T., and Kim, D. G. (2002) *J. Biol. Chem.* **277**, 3870–3877
17. Fawcett, T. W., Eastman, H. B., Martindale, J. L., and Holbrook, N. J. (1996) *J. Biol. Chem.* **271**, 14285–14289
18. You, K. R., Shin, M. N., Park, R. K., Lee, S. O., and Kim, D. G. (2001) *Hepatology* **34**, 1119–1127
19. Grutter, M. G. (2000) *Curr. Opin. Struct. Biol.* **10**, 649–655
20. Yang, J. C., and Cortopassi, G. (1998) *Free Radic. Biol. Med.* **24**, 624–631
21. Eymyn, B., Dubrez, L., Allouche, M., and Solary, E. (1997) *Cancer Res.* **57**, 686–695
22. McCullough, K. D., Martindale, J. L., Klotz, L. O., Aw, T. Y., and Holbrook, N. J. (2001) *Mol. Cell. Biol.* **21**, 1249–1259
23. Y Kito, M., Akao, Y., Ohishi, N., Yagi, K., and Nozawa, Y. (2002) *Biochem. Biophys. Res. Commun.* **291**, 861–867
24. Meister, A. (1988) in *Mechanisms of Drug Resistance in Neoplastic Cells* (Woolley, P. V., III, and Tew, K. D., eds) pp. 99–127, Academic Press, Inc., New York
25. Yokomizo, A., Kohno, K., Wada, M., Ono, M., Morrow, C. S., Cowan, K. H., and Kuwano, M. (1995) *J. Biol. Chem.* **270**, 19451–19457
26. Rao, P. N. (1980) *Mol. Cell. Biochem.* **29**, 47–57
27. Baeuerle, P. A., and Baltimore, D. (1996) *Cell* **87**, 13–20
28. Beg, A. A., and Baltimore, D. (1996) *Science* **274**, 782–784
29. Wang, C. Y., Mayo, M. W., and Baldwin, A. S., Jr. (1996) *Science* **274**, 784–787
30. Nozaki, S., Sledge, G. W., Jr., and Nakshatri, H. (2001) *Oncogene* **20**, 2178–2185
31. Patel, N. M., Nozaki, S., Shortle, N. H., Bhat-Nakshatri, P., Newton, T. R., Rice, S., Gelfanov, V., Boswell, S. H., Goulet, R. J., Jr., Sledge, G. W., Jr., and Nakshatri, H. (2000) *Oncogene* **19**, 4159–4169
32. Wang, C. Y., Mayo, M. W., Korneluk, R. G., Goeddel, D. V., and Baldwin, A. S., Jr. (1998) *Science* **281**, 1680–1683
33. Lee, H. H., Dadgostar, H., Cheng, Q., Shu, J., and Cheng, G. (1999) *Proc. Natl. Acad. Sci. U. S. A.* **96**, 9136–9141
34. Grumont, R. J., Rourke, I. J., and Gerondakis, S. (1999) *Genes Dev.* **13**, 400–411
35. Zong, W. X., Edelstein, L. C., Chen, C., Bash, J., and Gelinas, C. (1999) *Genes Dev.* **13**, 382–387
36. Jones, P. L., Ping, D., and Boss, J. M. (1997) *Mol. Cell. Biol.* **17**, 6970–6981
37. Zou, H., Li, Y., Liu, X., and Wang, X. (1999) *J. Biol. Chem.* **274**, 11549–11556
38. Li, P., Nijhawan, D., Budihardjo, I., Srinivasula, S. M., Ahmad, M., Alnemri, E. S., and Wang, X. (1997) *Cell* **91**, 479–489
39. Srinivasula, S. M., Ahmad, M., Fernandes-Alnemri, T., and Alnemri, E. S. (1998) *Mol. Cell* **1**, 949–957
40. Fulda, S., Scaffidi, C., Susin, S. A., Krammer, P. H., Kroemer, G., Peter, M. E., and Debatin, K. M. (1998) *J. Biol. Chem.* **273**, 33942–33948
41. Gately, D. P., Jones, J. A., Christen, R., Barton, R. M., Los, G., and Howell, S. B. (1994) *Br. J. Cancer* **70**, 1102–1106
42. Gately, D. P., and Howell, S. B. (1996) *J. Biol. Chem.* **271**, 20588–20593
43. Oberhammer, F., Wilson, J. W., Dive, C., Morris, I. D., Hickman, J. A., Wakeling, A. E., Walker, P. R., and Sikorska, M. (1993) *EMBO J.* **12**, 3679–3684
44. Kim, R., Ohi, Y., Inoue, H., Aogi, K., and Toge, T. (1999) *Anticancer Res.* **19**, 1779–1783
45. Guyton, K. Z., Xu, Q., and Holbrook, N. J. (1996) *Biochem. J.* **314**, 547–554
46. Guillet, G., Harmatha, J., Waddell, T. G., Philogene, B. J., and Arnason, J. T. (2000) *Photochem. Photobiol.* **71**, 111–115
47. Luethy, J. D., and Holbrook, N. J. (1994) *Cancer Res.* **54**, Suppl. 7, 1902–1906
48. Goto, S., Iida, T., Cho, S., Oka, M., Kohno, S., and Kondo, T. (1999) *Free Radic. Res.* **31**, 549–558
49. Groenewegen, W. A., and Heptinstall, S. (1990) *J. Pharm. Pharmacol.* **42**, 553–557
50. Zhang, W., Lawa, R. E., Hinton, D. R., Su, Y., and Couldwell, W. T. (1995) *Cancer Lett.* **96**, 31–35
51. O'Connor, P. M., Jackman, J., Bae, I., Myers, T. G., Fan, S., Mutoh, M., Scudiero, D. A., Monks, A., Sausville, E. A., Weinstein, J. N., Friend, S., Fornace, A. J., Jr., and Kohn, K. W. (1997) *Cancer Res.* **57**, 4285–4300
52. Friedman, A. D. (1996) *Cancer Res.* **56**, 3250–3256
53. Picman, A. K., Rodriguez, E., and Towers, G. H. (1979) *Chem. Biol. Interact.* **28**, 83–89
54. Arrick, B. A., Nathan, C. F., and Cohn, Z. A. (1983) *J. Clin. Invest.* **71**, 258–267
55. Woerdenbag, H. J., Lemstra, W., Malingre, T. M., and Konings, A. W. (1989) *Br. J. Cancer* **59**, 68–75
56. Anderson, M. E., and Meister, A. (1983) *Proc. Natl. Acad. Sci. U. S. A.* **80**, 707–711
57. Tew, K. D. (1994) *Cancer Res.* **54**, 4313–4320
58. Saburi, Y., Nakagawa, M., Ono, M., Sakai, M., Muramatsu, M., Kohno, K., and Kuwano, M. (1989) *Cancer Res.* **49**, 7020–7025